

Cellular Injury Associated with Renal Thrombotic Microangiopathy in Human Immunodeficiency Virus–Infected Macaques

STEPHAN SEGERER,* FRANK EITNER,[†] YAN CUI,* KELLY L. HUDKINS,* and CHARLES E. ALPERS*

*Department of Pathology, University of Washington, Seattle, Washington; and [†]Division of Nephrology, University of Aachen, Aachen, Germany.

Abstract. Pigtailed macaques infected with a virulent human immunodeficiency virus-2 (HIV-2) strain develop renal thrombotic microangiopathy (TMA), which morphologically resembles aspects of human HIV-associated TMA. Apoptotic cell death of microvascular endothelial cells might be a pathogenetic clue to this disease. For defining further the pattern of cellular injury in this model, serial kidney sections of 58 macaques infected with HIV-2 and 7 uninfected controls were studied by routine microscopy, terminal deoxynucleotidyl-transferase-mediated dUTP nick-end labeling (TUNEL), 4',6-diamidino-2-phenylindole staining, and immunohistochemistry for single-stranded DNA, p53, the Wilms' tumor suppressor gene-1 peptide product, caspase-3, and the proliferation marker Ki67. Selected cases were further evaluated by *in situ* end labeling and transmission electron microscopy. Kidneys of 13

HIV-2–infected animals contained a pattern of cellular injury, which was characterized by (1) nuclear swelling with an ultrastructural morphology different from apoptotic nuclei, (2) sharply demarcated areas of renal cells with chromatin nicks (TUNEL positive) and single-stranded DNA, (3) absence of an inflammatory or proliferative response, (4) upregulation of p53 and loss of at least one cellular differentiation marker (Wilms' tumor suppressor gene-1), (5) a tight correlation with the diagnosis of renal TMA, and (6) a contrast between profound changes in the renal cellular morphology and the apparently unaffected clinical condition of the host. This pattern of injury, which shares some features of both apoptotic and oncotic necrosis, might be involved in the pathogenesis of HIV-associated renal TMA in this model.

Apoptotic cell death has been defined as a crucial event in organ development, regulation of the immune system, and in a variety of tissue injuries, which brought renewed interest to the nomenclature and characterization of cell death (1–5). Apoptosis is a controlled form of cell suicide, which is morphologically characterized by nuclear condensation (pyknosis) and breaking up of the nucleus into membrane-bound fragments, karyorrhexis (6,7). Despite the precision achieved in defining some pathways of apoptotic cell death in well-controlled cell systems, our ability to recognize, define, and distinguish it from other forms of cell injury and cell death in the setting of tissue injury *in vivo* remains problematic (8–10). A pitfall of morphologic studies results from the rapid disappearance of apoptotic cells via phagocytosis by professional and nonprofessional phagocytes (9,11). This efficient process leads to a small number of cells with an apoptotic appearance at a given time in tissue and therefore might result in underestimation of the contribution of apoptotic cell death (12).

An even more fundamental problem arises in the attempt to clearly define apoptosis and distinguish it from other forms of cell death (13). Currently, the evaluation of apoptotic cell death in tissue sections relies on the combination of techniques that demonstrate typical but nonspecific features of apoptotic cells (*e.g.*, DNA strand breaks) with the morphology by light and/or electron microscopy.

The association between human immunodeficiency virus (HIV) infection and thrombotic microangiopathy (TMA) has been increasingly recognized (14). Endothelial cell apoptosis has been implicated in the pathogenesis of HIV-associated TMA in humans as plasma obtained from patients with this disorder induces apoptosis, as well as procoagulant properties in cultured endothelial cells (15–17). We demonstrated that infection of pigtailed macaques with a virulent HIV-2 strain resulted in renal TMA, defined by thrombi in arterioles and glomerular capillaries, in approximately 20% of the animals (18). The lesion closely resembles the morphology seen in the human disease. In the present study, we evaluated the renal pathology using markers of DNA strand breaks, proliferation, renal cell phenotype, and ultrastructural appearance. Consistent with previous reports in humans, we found an increased number of terminal deoxynucleotidyl-transferase-mediated dUTP nick-end labeling (TUNEL)-positive cells. However, as detailed below, the pattern of injury and the morphology were not consistent with the classical description of apoptotic cell death.

Received April 16, 2001. Accepted August 23, 2001.

Address correspondence to Dr. Charles Alpers, Department of Pathology, University of Washington, Medical Center, Box 357470, 1959 NE Pacific Street, Seattle, WA 98195. Phone: 206-543-5616; Fax: 206-543-3644; E-mail: calp@u.washington.edu

1046-6673/1302-0370

Journal of the American Society of Nephrology

Copyright © 2002 by the American Society of Nephrology

Materials and Methods

Tissue Samples

Renal specimens of 65 pigtailed macaques were included in the study. Fifty-eight macaques were infected with HIV-2, and 7 uninfected macaques served as normal controls. The mean time of infection was 187 d, ranging from periods between 0.5 and 1877 d. Only two animals were infected for longer than 2 yr. The histologic lesions resembling renal TMA in the studied animals have previously been described in detail (18). See the Analysis of the Material section for the definitions used to describe the lesion in the present study.

Kidneys were fixed in 10% neutral buffered formalin or in methyl Carnoy's solution (60% methanol, 30% chloroform, 10% acetic acid) and routinely embedded in paraffin. From each formalin-fixed tissue block, serial sections were cut at 4 μ m. Tissue for electron microscopy was fixed in half-strength Karnovsky's solution (1% paraformaldehyde and 1.25% glutaraldehyde in 0.1 M Na cacodylate buffer [pH 7.0]).

Detection of DNA Fragments, Single-Stranded DNA, and Condensed Nuclei

For the detection of DNA fragments by TUNEL methodology, we used the TdT-FragEL DNA Fragmentation Detection Kit (Oncogene Research Products, Boston, MA). A second TUNEL kit, based on the incorporation of a brominated nucleotide and the detection by an anti-brominated nucleotide antibody, was used in 15 cases (TACS · XL-DAB, Trevigen, Gaithersburg, MD). *In situ* end labeling, based on the Klenow enzyme, was used in a series of 31 specimens (KLENOW-FragEL DNA Fragmentation Detection Kit, Oncogene Research Products). The materials were used according to the instructions of the manufacturer with minor modifications. For the TdT-FragEL DNA Fragmentation Detection Kit, the protocol is described in brief. Deparaffinized and rehydrated slides were rinsed in TBS (140 mM NaCl, 20 mM Tris [pH 7.6]) and incubated in Proteinase K (20 μ g/ml in 10 mM Tris [pH 8]; Oncogene Research Products) for 20 min at room temperature. Endogenous peroxidases were blocked by a 5-min incubation in 3% H₂O₂ in methanol and slides were incubated with equilibration buffer for 30 min. Sixty microliters of TdT Labeling Reaction Mixture containing 3 μ l of TdT was added for 60 min. Specimens were incubated in Stop Solution for 5 min, followed by a rinse in TBS. Slides were incubated in blocking buffer for 5 min, followed by an incubation with the ABC Reagent (Vector, Burlingame, CA). Color development was performed applying diaminobenzidine (Sigma, St. Louis, MO) with Nickel enhancement. Slides were counterstained with methyl green, dehydrated, and coverslipped. Negative controls were performed by omitting TdT, and positive controls were performed by digestion with DNase.

A monoclonal antibody F7-26 (Chemicon, International, Inc., Temecula, CA) can be used to detect single-stranded DNA (ssDNA) after thermal denaturation (19,20). The monoclonal antibody F7-26 was used according to the instructions of the manufacturer. A peroxidase-conjugated monoclonal rat anti-mouse IgM antibody (Zymed, San Francisco, CA) was used as secondary reagent. The color reaction was performed as described above.

For the detection of condensed nuclei 4',6-diamidino-2-phenylindole (DAPI) staining was used. Slides from formalin-fixed and paraffin-embedded tissue were deparaffinized and coverslipped with Vectashield Mounting Medium with DAPI (Vector).

Immunohistochemistry

We previously described the immunohistochemical techniques used in this study in detail (21–23). The specificities of the monoclo-

nal mouse anti-p53 antibody (clone BP53-12; Sigma), the polyclonal rabbit anti-Wilms' tumor suppressor gene-1 (WT-1; C-19; Santa Cruz Biotechnology, Inc., Santa Cruz, CA), and the monoclonal mouse anti-Ki67 antibody (MIB-1; Amac Inc., Westbrook, ME) have all been previously shown by immunoblotting, and the application for immunohistochemistry has been published as well (24–28). The specificity of the polyclonal rabbit anti-active caspase-3 (Pharmingen, San Diego, CA) antibody has been tested by immunoblotting by the company.

Analysis of the Material

A blinded observer evaluated 100 consecutive glomeruli for each specimen and staining technique. Glomeruli were categorized as positive when more than one tenth of the glomerular cells were involved. Glomeruli with <5 WT-1 positive cells were labeled as having reduced WT-1 expression. Five or more p53-positive cells within a glomerulus was the definition of a p53-positive glomerulus. Ki67-positive cells were counted per glomerulus and per cortical field (measuring 0.0625 mm²).

Apoptosis was quantified on DAPI stains. Bright round condensed nuclei were counted as a feature of classical apoptosis in 30 high-power fields at a magnification of \times 1000. The InStat program (Version 3.0 for Windows; Intuitive Software for Science, San Diego, CA) was used to calculate the two-tail *P* value (Fisher's exact test), the Spearman rank correlation, and the nonparametric Kruskal-Wallis test for comparison of means.

Results

HIV-2-Infected Macaques Develop Areas of TUNEL-Positive Cells in the Kidney

We studied renal specimens from a total of 58 HIV-2-infected pigtailed macaques and 7 uninfected controls. We identified renal TMA in 13 HIV-2-infected animals (18). In two additional specimens, both from HIV-2-infected macaques, the morphology was suggestive of TMA, with focal thickening and double contours of glomerular capillaries and endothelial swelling but without overt thrombi. These two cases were classified as indeterminate. Therefore, of the 58 infected macaques, 13 were classified as having TMA, 2 as indeterminate, and 43 as having no renal TMA.

Areas of TUNEL-positive cells were found in 13 of 65 renal specimens (20%) in a blinded evaluation. Two different patterns of TUNEL positivity were distinguishable (Figure 1). In 10 cases, the nuclei of all cell types within broad areas of tissue, which appeared centered around arteries, were swollen and TUNEL positive (arterial pattern, Figure 1, A through D). Involved were cells of the arterial walls, adjacent veins, adjacent tubular epithelium, and adjacent whole glomeruli (Figure 2, compared with normal in Figure 3). The arterial pattern was usually widespread, with a mean of 51 of 100 glomeruli involved (range, 21% to 72%; Figure 1, A and B).

Besides the widespread arterial pattern, three cases demonstrated small areas of TUNEL-positive cells involving large veins, the adjacent tubular epithelium, and rarely parts of adjacent glomeruli (venous pattern; Figure 1, E and F). Adjacent arteries showed no TUNEL-positive nuclei in these cases (Figure 1F). The border between involved tissue with TUNEL-positive nuclei and adjacent normal renal tissue was strikingly

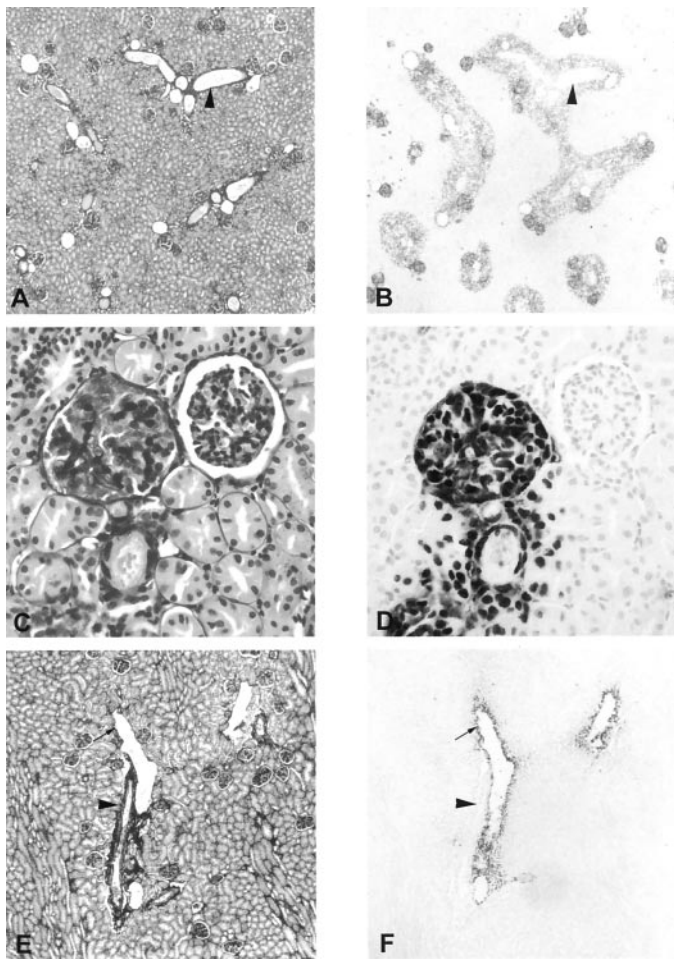


Figure 1. Different patterns of TUNEL-positive areas in HIV-2-infected macaques with renal TMA. (A and B) Renal specimen from an HIV-2-infected macaque with TMA stained by silver methenamine and TUNEL. Note the widespread involvement of renal tissue (B) and the sharp demarcation of the process. The arterial pattern involves arteries (arrowhead), surrounding tubular epithelium and whole glomeruli (D). Note the TUNEL-negative glomerulus with normal nuclear features (right) adjacent to the involved glomerulus (left, C and D). (E and F) Renal specimen from an HIV-2-infected macaque stained by silver methenamine and TUNEL. Only small areas of the kidney, including larger veins and the adjacent tubular cells, are involved (arrow, venous pattern). The arrowhead marks an artery adjacent to the involved vein, which is TUNEL negative (E, F). Magnifications: $\times 40$ in A, B, E, and F; $\times 400$ in C and D.

demarcated (*i.e.*, the injury was identifiable as a field defect; Figures 1, B and F, and 4). In selected cases, these results were confirmed with additional end-labeling techniques, which are based on different enzymes, different incorporated nucleotides, and different detection systems. The distribution pattern was virtually identical with all techniques.

The described findings were substantiated by immunohistochemistry for ssDNA, a technique that is not based on end labeling of DNA strand breaks. Staining for ssDNA showed an arterial pattern in all 10 cases, and 3 cases showed a venous distribution, 2 of which demonstrated the same pattern in the

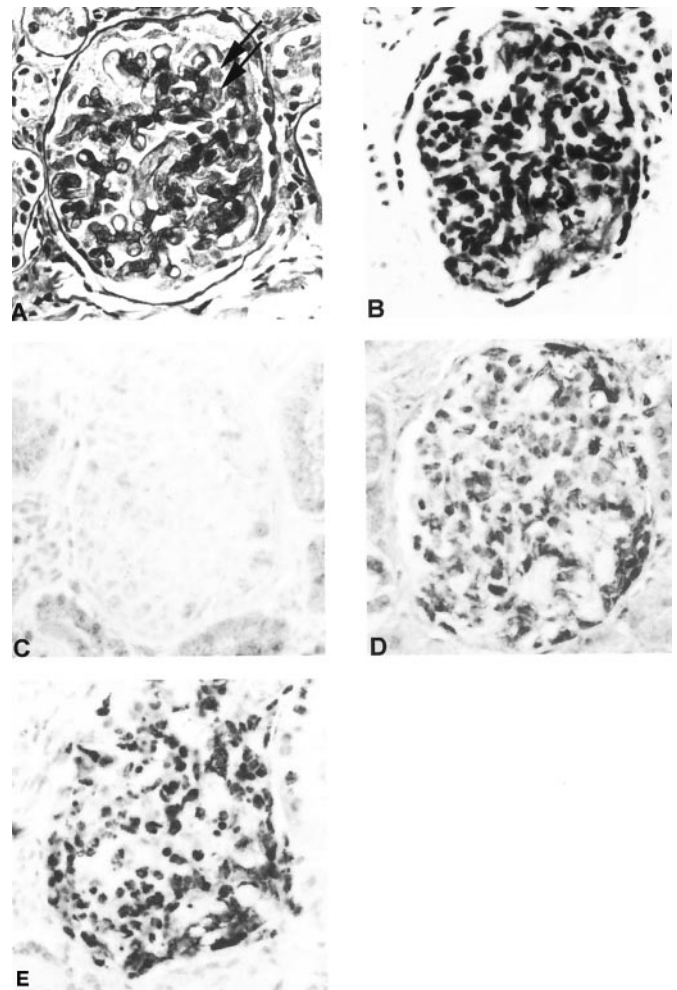


Figure 2. Glomerulus with TUNEL-positive cells. Consecutive sections of a renal specimen from an HIV-2-infected macaque with TMA were stained with periodic acid-Schiff (PAS; A) and TUNEL (B), and immunohistochemistry for WT-1 (C), p53 (D), and ssDNA (E) were performed. Nuclei were swollen and pale on the PAS stain (A, arrows). All glomerular cells were TUNEL positive (B). WT-1 expression was completely absent (C). The nuclei of the glomerular cells were positive for p53 (D) and ssDNA (E). Magnification, $\times 400$.

TUNEL stain. The correlation between the percentage of positive glomeruli for ssDNA and for TUNEL was highly significant ($r = 0.97$, $P < 0.0001$, $n = 62$).

In kidneys from uninfected control macaques, only a small number of scattered positive nuclei in the interstitium between tubular cells, in tubular epithelium, in leukocytes within the lumen of arteries, and rarely within glomeruli were TUNEL positive. The number and distribution are consistent with apoptotic cells in normal human kidneys as described previously (29).

Areas of TUNEL-Positive Cells Are Almost Exclusively Found in Specimens with Renal TMA

A striking finding was that the 13 cases with TUNEL-positive areas included 10 cases with TMA and the 2 indeterminate cases. All specimens with the arterial pattern and two of

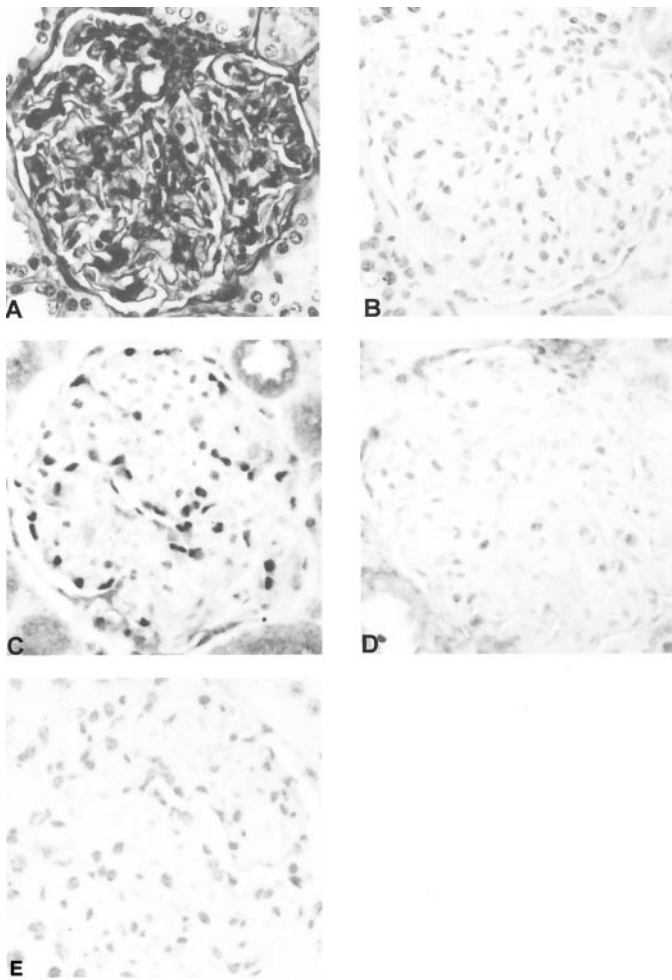


Figure 3. Representative normal glomerular staining pattern. Consecutive sections of a renal specimen from an uninfected macaque were stained with PAS (A) and TUNEL (B), and immunohistochemistry for WT-1 (C), p53 (D), and ssDNA (E) were performed. The illustrated glomerulus shows WT-1 expression in the podocytes but no glomerular TUNEL-, p53-, or ssDNA-positive cells (compared with Figure 2). Magnification, $\times 400$.

three with the perivenous pattern were from cases with TMA. The association between TMA and cases with TUNEL-positive areas was highly significant ($P < 0.0001$). When the indeterminate cases were considered as normal, the sensitivity of the presence of TUNEL-positive areas for the diagnosis of renal TMA was 0.77, the specificity 0.94, the positive predictive value was 0.77, and the negative predictive value was 0.94. When the indeterminate cases were considered as abnormal, the sensitivity was 0.8, the specificity was 0.98, the positive predictive value rose to 0.92, and the negative predictive value was 0.94.

Ultrastructure of Nuclei in TUNEL-Positive Areas Is Different from Both Apoptotic and Oncotic Necrosis

The most prominent histologic change was severe swelling and a pale appearance of nuclei on silver stains (Figures 1, C and D, and 2). On DAPI stains, cells with condensed, bright

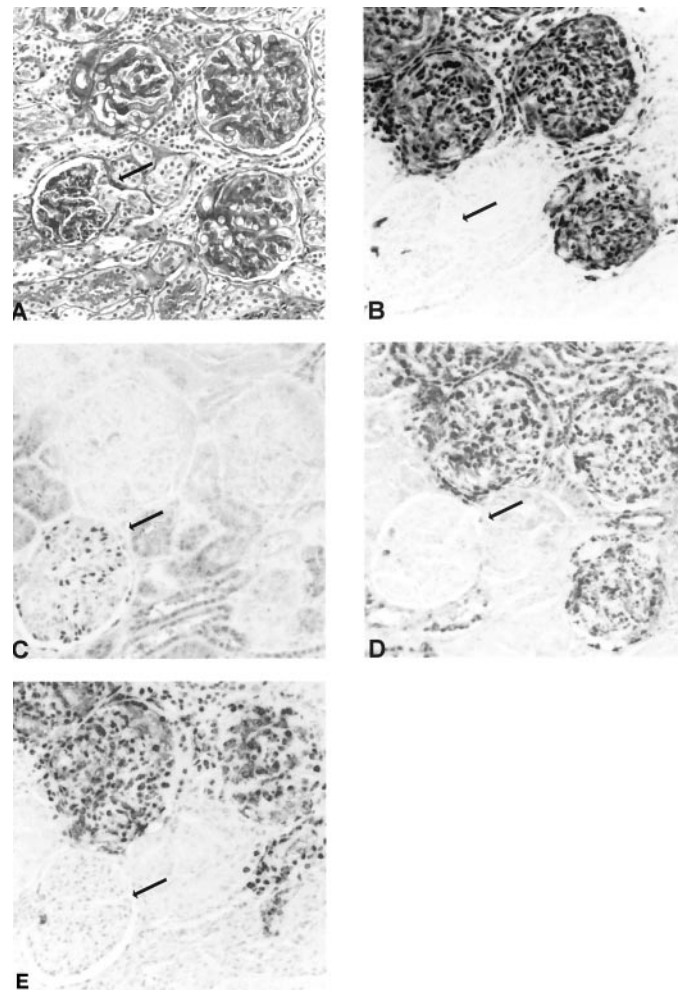


Figure 4. Changes in protein expression in TUNEL-positive areas. Consecutive sections of a renal specimen from a HIV-2-infected macaque with TMA were stained with PAS (A) and TUNEL (B), and immunohistochemistry for WT-1 (C), p53 (D), and ssDNA (E) were performed. This figure illustrates the involvement of three glomeruli and one adjacent normal glomerulus in the left lower quadrant (arrow). The three involved glomeruli show the typical features with nuclear swelling (A), strong TUNEL (B), p53 (D), and ssDNA positivity (E). WT-1 is absent in the involved glomeruli but is present in the normal glomerulus (C). Magnification, $\times 400$.

nuclei were very rare. We found no differences between the groups in the number of nuclei with this classical feature of apoptosis (data not shown).

Using the feature of swollen, pale nuclei in glomeruli in a blinded evaluation, we found an excellent correlation between the percentage of glomeruli with more than one tenth of the glomerular nuclei positive for TUNEL and nuclear alterations detected in periodic acid-Schiff ($r = 0.88$, $P < 0.0001$, $n = 65$) or silver stains ($r = 0.97$, $P < 0.0001$, $n = 58$). The sharply demarcated areas of TUNEL positivity demonstrated no surrounding inflammatory reaction.

By transmission electron microscopy, nuclei involved in TUNEL-positive areas were swollen and contained two patterns of chromatin organization. The nuclear center had a

speckled but homogeneous electron density (Figure 5A, compared with the normal nuclei in Figure 5B). The rest of the nuclear area was electron lucent and contained small electron-dense bodies that had the appearance of condensed chromatin (Figure 5A, insert). Therefore, the normal nuclear ultrastructure with the electron-dense heterochromatin in the periphery was no longer apparent (Figure 5B). Tubuli with normal nuclear features were found next to glomeruli with the described ultrastructural features (Figure 5, arrow). All involved cell types, *i.e.*, glomerular cells, endothelial cells, myocytes of vessel walls, and tubular epithelium, demonstrated the same ultrastructural features (Figures 5 and 6). Venous endothelial

cells with these nuclear features were sometimes detached from the basal membrane (Figure 6A). Effacement of podocyte foot processes was found in glomeruli, where podocytes showed these nuclear changes (Figure 5A).

Podocytes in TUNEL-Positive Areas Lose the Constitutive Expression of WT-1

WT-1 plays a crucial role during nephrogenesis; is constitutively expressed in mature, differentiated podocytes; and

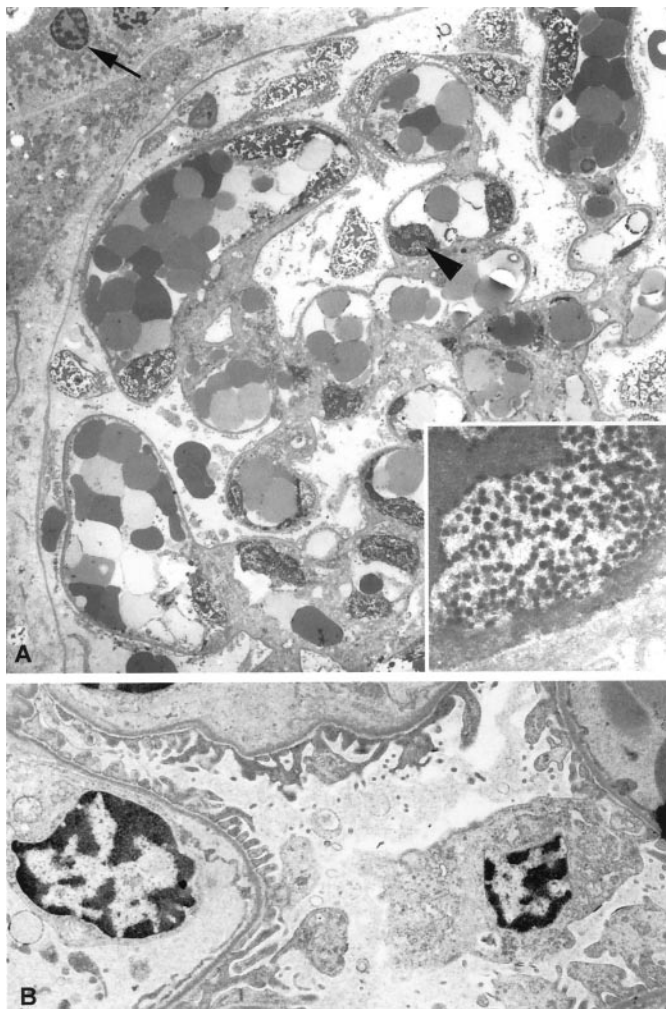


Figure 5. Ultrastructural features of glomeruli from a specimen with TUNEL-positive areas. Electron microscopy of a specimen from an HIV-2-infected macaque with TMA. (A) All different cell types of the glomerulus show nuclear swelling and nuclear changes. Note the normal nuclear appearance of the adjacent tubular epithelial cells (arrow). (Insert) Nuclear ultrastructural features of the nucleus of an endothelial cell (arrowhead) at high magnification. It contains a speckled but homogeneous organization of the center, surrounded by small, round, electron-dense particles. (B) Conserved glomerulus with normal nuclear ultrastructure from the same specimen as illustrated in A. Magnifications: $\times 800$ in A; $\times 10,000$ in A insert; $\times 2400$ in B.

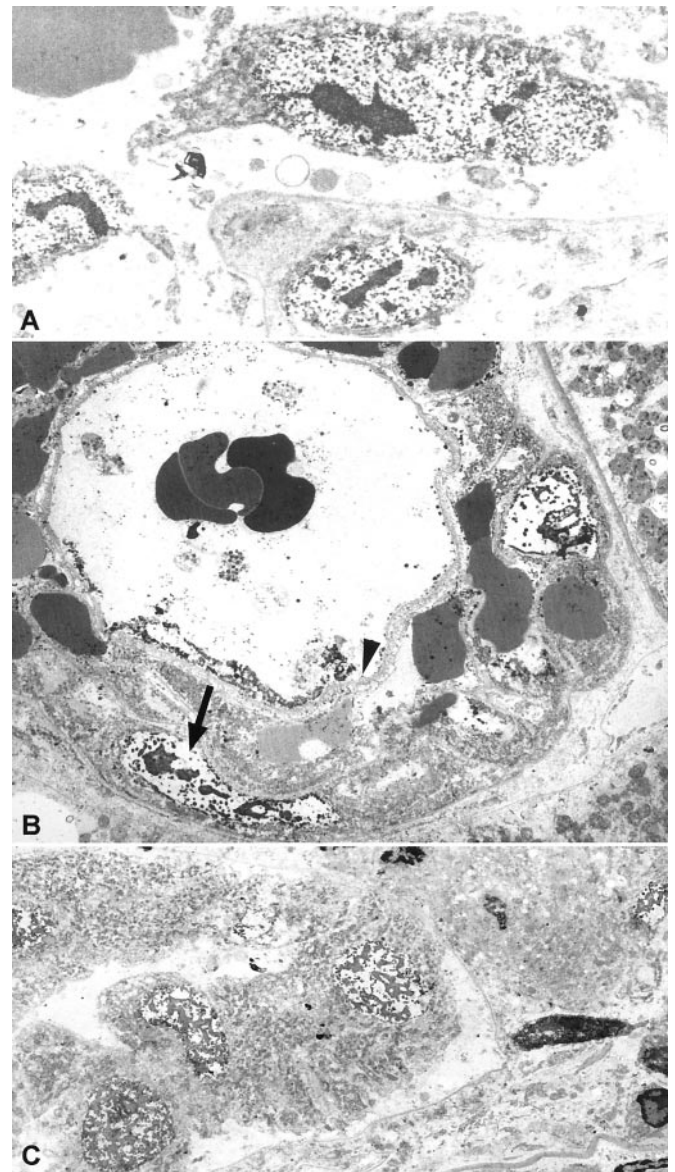


Figure 6. Ultrastructural features of veins, arteries, and epithelium in TUNEL-positive areas. Specimens from HIV-2-infected macaques with TMA. (A) Detachment of an endothelial cell with the described nuclear ultrastructural features. (B) Vascular wall of a small artery. Myocytes of the vessel wall show the typical nuclear features (arrow). Note red blood cells in the arterial wall. No endothelial cells are apparent covering the elastica interna (arrowhead). (C) Tubular epithelial cells in TUNEL-positive areas sometimes appeared detached from the basal membrane. Magnifications: $\times 2400$ in A; $\times 1600$ in B and C.

accordingly serves as a useful phenotypic marker of these cells (Figure 3C) (26,30). WT-1 was absent in glomeruli in TUNEL-positive areas but was expressed in adjacent normal glomeruli (Figures 2C and 4C). Decreased glomerular WT-1 expression was found in all cases with the arterial pattern and in one case with the perivenous distribution of TUNEL-positive cells. The correlation between the percentage of glomeruli with reduced WT-1 expression and TUNEL-positive glomeruli was highly significant ($r = 0.84$, $P < 0.0001$, $n = 64$).

p53 Is Expressed and No Proliferative or Inflammatory Response Is Present in TUNEL-Positive Areas

Glomerular cells in control specimens did not express p53 (Figure 3). Nuclear p53 expression was detected in all 10 cases with the arterial pattern in the same distribution as the TUNEL-positive cells (Figure 4). Five cases without TUNEL-positive areas contained p53-positive cells with a normal nuclear morphology on replicate tissue sections. All five of these specimens were from HIV-2-infected animals.

Both HIV-2-infected and normal control specimens contained a low number of proliferating cells in tubular epithelium, in the interstitium between tubules, and occasionally in glomeruli. A higher number of Ki67-expressing cells were found at sites of focal leukocytic infiltration. Animals with TUNEL-positive areas contained a significantly lower number of Ki67-positive cells per glomerulus compared with the group of HIV-2-infected animals without these areas (0.27 ± 0.09 versus 0.81 ± 0.13 ; $P < 0.05$; Figure 7). Specimens from HIV-2-infected animals showed a trend toward higher numbers of Ki67-positive cells, but the differences compared with normal animals did not reach statistical significance (Figure 7). TUNEL-positive areas were not associated with inflammatory infiltrates.

The available measurements of serum creatinine (0.67 mg/dl [$n = 38$] versus 0.64 mg/dl [$n = 10$]) and blood urea nitrogen (26.3 mg/dl [$n = 40$] versus 28.5 mg/dl [$n = 11$]) did not differ between cases without and with TUNEL-positive areas. None of the animals had clinical signs of impaired renal function or systemic illness. The strain of HIV-2 used is pathogenic for an acquired immunodeficiency syndrome–like syndrome in macaques at time points later than those used in the prospective serial sacrifice portion of the study. These manifestations, like the human disease that they model, may occur months to years after infection and are not invariably present as some macaques have survived >3 yr without clinical symptoms despite documented infections.

Discussion

The pathogenesis of TMA in retrovirus-infected individuals is still obscure. Plasma from patients with acute thrombotic thrombocytopenic purpura, with and without HIV infection, has been shown to induce apoptosis in microvascular endothelial cells but not in endothelial cells of large-vessel origin (15). A differential induction of apoptosis by plasma from patients with TMA in dermal, renal, and cerebral microvascular endothelium (*i.e.*, sites typically affected by TMA) but not in endothelial cells of pulmonary and hepatic origin (*i.e.*, sites

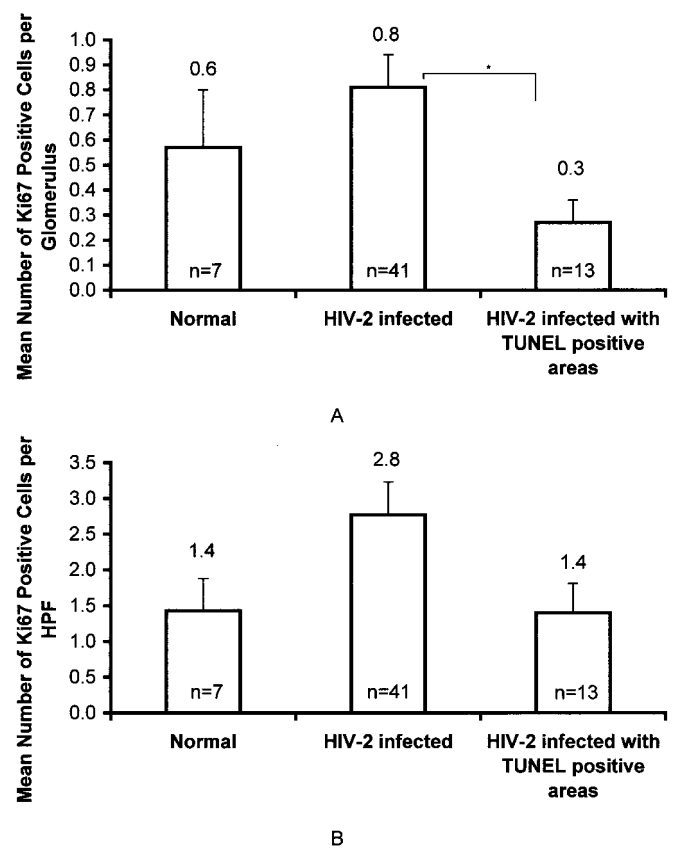


Figure 7. Expression of the proliferation marker Ki67. Mean number of Ki67-positive cells per glomerulus (A) and per high-power field (HPF; B) in uninfected macaques, macaques with HIV-2 infection, and macaques with HIV-2 infection and TUNEL-positive areas (Bars give SEM; * $P < 0.05$)

typically not affected by TMA) has been reported (31). In addition, increased numbers of TUNEL-positive microvascular endothelial cells were described in spleens from patients with TMA (32). Recent studies identified potential links between endothelial cell apoptosis and initiation of a procoagulant phenotype, which included decreased production of prostaglandin I_2 , increased procoagulant surface plebs, increased tissue factor activity, and decreased anticoagulant factors (thrombomodulin, heparan sulfate, tissue factor pathway inhibitor) (16,17,31). These reports prompted us to conduct the current study on the pattern of cellular injury in HIV-2-infected macaques with renal TMA using ultrastructural analysis in combination with markers of DNA injury, cell proliferation, and cellular phenotype. Increasing evidence suggests that the classical modes of cell death, apoptosis, and oncosis (summarized in a simplified way in Table 1) represent only the extreme ends of a range of morphologic representations of cell death (12). We describe a pattern of cellular injury that shares features of both classical forms of cell death (Table 1) (13,33). Markers of DNA strand breaks demonstrated a positive reaction in sharply demarcated areas of renal tissue. This distribution pattern involving areas of different cells fits to an oncotic lesion rather than an apoptotic form of cell death, which usually can be detected only in

Table 1. Comparison between the pattern of injury in HIV-2–infected macaques with the features of apoptotic and oncotic necrosis

	Oncosis	Apoptosis	Cellular Injury in HIV-2–Infected Macaques
Nuclei	Swelling Pale Karyolysis	Shrinkage Dense Karyorrhexis	Swelling Pale
Cell	Swelling Disintegration	Segregation into “apoptotic bodies”	?
Chromatin	Irregular clumps (coarse strand)	Condensation into blebs near the nuclear envelope	Condensation into a dense center, surrounded by condensed small particles
Distribution	Groups of cells	Single cells	Groups of cells
Inflammation	Yes	No	No
TUNEL	Positive	Positive	Positive
ssDNA	? (antibody dependent)	Positive	Positive

a low number of scattered single cells in tissue sections (7,12,34). The absence of an inflammatory response, however, is in stark contrast with an oncotic lesion, in which the spill of cytoplasmic content leads to an inflammatory response (13,33,35). A principle morphologic feature that separates this lesion from apoptosis is the nuclear swelling (Figure 1) (33). We could not detect active caspase 3 in the lesion. This finding is consistent with either a nonapoptotic pathway or a stage of apoptosis in which caspase 3 is not activated.

Are cells in TUNEL-positive areas doomed to die? The profound morphologic changes and the DNA nicks, indicated by the strong staining by the TUNEL method, might suggest a lethal injury. By electron microscopy, the nuclei show two patterns of chromatin organization, with a central region of high electron density, which is surrounded by an electron-lucent area filled with small electron-dense particles. This ultrastructural morphology is distinguishable from both of the conventional, well-described forms of cell death discussed previously. However, the contrast between the large areas of injury, the absence of clinical symptoms, and the absence of residual or progressive lesions suggest a sublethal insult.

The described pattern of injury was tightly associated with the morphologic diagnosis of TMA. The 10 cases with an arterial distribution pattern of TUNEL-positive areas were from 8 animals with TMA and the 2 indeterminate cases. None of the noninfected controls demonstrated TUNEL-positive areas. TUNEL positivity of endothelial cells might provide a pathophysiologic clue for understanding the pathogenesis of TMA in this model. A morphologic hint of a potential prothrombotic surface is the observation of endothelial cells detached from basement membranes and hence exposing extracellular matrices, which might then serve as procoagulant sites in affected vessels (36).

Studies on the appearance of endothelial cells in patients with thrombotic microangiopathies demonstrated swollen endothelial cells commonly separated from the basement membrane with ruffled endothelial surface and pseudopodal extensions (32,37,38). Other nonspecific findings were increased mitochondria, enlarged Golgi elements, and numerous lyso-

somes (reviewed in Kwaan (38)). In spleens from patients with thrombotic thrombocytopenic purpura, TUNEL-positive endothelial cells and hyperchromatic nuclei were described (32). We found that endothelial cells were commonly detached from the basement membrane and demonstrated the described nuclear features not consistent with classical apoptosis. Some of the endothelial features described in the literature are consistent with apoptotic cell death, but further ultrastructural studies are needed to define clearly the pattern of endothelial injury in humans with renal TMA.

The tumor-suppressor gene p53 accumulates and is activated by various forms of DNA damage and may cause either cell-cycle arrest or apoptosis (reviewed in May and May (39)). The increased glomerular expression of p53 in TUNEL-positive areas in combination with decreased cell proliferation, illustrated by significantly decreased numbers of glomerular Ki67-positive cells, is consistent with a p53-induced cell-cycle arrest. The absence of WT-1 in TUNEL-positive glomeruli illustrates the profound phenotypic change of cells involved in this type of injury. We have no reason to believe that this last change is functionally implicated in the TMA injury, but decreased expression of WT-1 has been described in humans with HIV-associated nephropathy (26).

Although the TUNEL method has been widely used both in animal studies and on human tissue, the features described here in aggregate have previously not been recognized and are currently restricted to retrovirus-infected primates. Additional studies need to address whether this pattern of injury is related to TMA in the context of HIV or to HIV infection itself or whether this might be a cellular reaction specific for the primate response to retrovirus-associated renal TMA. The cellular reaction furthermore has to be defined as a certain stage of cell death or a form of cell and tissue injury, which might potentially be reversible. Our limitation to fixed tissue excluded *in vitro* experiments to answer these questions.

Acknowledgments

This work was supported by Grants HL63652 and RR00166 from the National Institutes of Health and by a grant from the Else Kröner-

Fresenius-Stiftung (Bad Homburg v. d. Höhe, Germany). We thank Min Wen for assistance with electron microscopy.

References

1. Hammerman MR: Regulation of cell survival during renal development. *Pediatr Nephrol* 12: 596–602, 1998
2. Sebzda E, Mariathasan S, Ohteki T, Jones R, Bachmann MF, Ohashi PS: Selection of the T cell repertoire. *Annu Rev Immunol* 17: 829–874, 1999
3. Ueda N, Kaushal GP, Shah SV: Apoptotic mechanisms in acute renal failure. *Am J Med* 108: 403–415, 2000
4. Owen-Schaub L, Chan H, Cusack JC, Roth J, Hill LL: Fas and Fas ligand interactions in malignant disease. *Int J Oncol* 17: 5–12, 2000
5. Levin S, Bucci TJ, Cohen SM, Fix AS, Hardisty JF, LeGrand EK, Maronpot RR, Trump BF: The nomenclature of cell death: Recommendations of an ad hoc Committee of the Society of Toxicologic Pathologists. *Toxicol Pathol* 27: 484–490, 1999
6. Zamzami N, Kroemer G: Condensed matter in cell death. *Nature* 401: 127–128, 1999
7. Kerr JF, Wyllie AH, Currie AR: Apoptosis: A basic biological phenomenon with wide-ranging implications in tissue kinetics. *Br J Cancer* 26: 239–257, 1972
8. Reed JC: Mechanisms of apoptosis. *Am J Pathol* 157: 1415–1430, 2000
9. Willingham MC: Cytochemical methods for the detection of apoptosis. *J Histochem Cytochem* 47: 1101–1110, 1999
10. Darzynkiewicz Z, Bedner E, Traganos F, Murakami T: Critical aspects in the analysis of apoptosis and necrosis. *Hum Cell* 11: 3–12, 1998
11. Searle J, Kerr JF, Bishop CJ: Necrosis and apoptosis: Distinct modes of cell death with fundamentally different significance. *Pathol Annu* 17: 229–259, 1982
12. Leist M, Nicotera P: The shape of cell death. *Biochem Biophys Res Commun* 236: 1–9, 1997
13. Majno G, Joris I: Apoptosis, oncosis, and necrosis. An overview of cell death. *Am J Pathol* 146: 3–15, 1995
14. Hymes KB, Karpatkin S: Human immunodeficiency virus infection and thrombotic microangiopathy. *Semin Hematol* 34: 117–125, 1997
15. Laurence J, Mitra D, Steiner M, Staiano-Coico L, Jaffe E: Plasma from patients with idiopathic and human immunodeficiency virus-associated thrombotic thrombocytopenic purpura induces apoptosis in microvascular endothelial cells. *Blood* 87: 3245–3254, 1996
16. Bombeli T, Karsan A, Tait JF, Harlan JM: Apoptotic vascular endothelial cells become procoagulant. *Blood* 89: 2429–2442, 1997
17. Casciola-Rosen L, Rosen A, Petri M, Schlissel M: Surface blebs on apoptotic cells are sites of enhanced procoagulant activity: Implications for coagulation events and antigenic spread in systemic lupus erythematosus. *Proc Natl Acad Sci USA* 93: 1624–1629, 1996
18. Eitner F, Cui Y, Hudkins KL, Schmidt A, Birkebak T, Agy MB, Hu SL, Morton WR, Anderson DM, Alpers CE: Thrombotic microangiopathy in the HIV-2-infected macaque. *Am J Pathol* 155: 649–661, 1999
19. Frankfurt OS: Detection of apoptosis in leukemic and breast cancer cells with monoclonal antibody to single-stranded DNA. *Anticancer Res* 14: 1861–1869, 1994
20. Frankfurt OS, Krishan A: Identification of apoptotic cells by formamide-induced DNA denaturation in condensed chromatin. *J Histochem Cytochem* 49: 369–378, 2001
21. Alpers CE, Hudkins KL, Davis CL, Marsh CL, Riches W, McCarty JM, Benjamin CD, Carlos TM, Harlan JM, Lobb R: Expression of vascular cell adhesion molecule-1 in kidney allograft rejection. *Kidney Int* 44: 805–816, 1993
22. Hudkins KL, Giachelli CM, Eitner F, Couser WG, Johnson RJ, Alpers CE: Osteopontin expression in human crescentic glomerulonephritis. *Kidney Int* 57: 105–116, 2000
23. Segerer S, Cui Y, Hudkins KL, Goodpaster T, Eitner F, Mack M, Schlondorff D, Alpers CE: Expression of the chemokine monocyte chemoattractant protein-1 and its receptor chemokine receptor 2 in human crescentic glomerulonephritis. *J Am Soc Nephrol* 11: 2231–2242, 2000
24. Bartkova J, Bartek J, Lukas J, Vojtesek B, Staskova Z, Rejthar A, Kovarik J, Midgley CA, Lane DP: p53 protein alterations in human testicular cancer including pre-invasive intratubular germ-cell neoplasia. *Int J Cancer* 49: 196–202, 1991
25. Bartek J, Bartkova J, Vojtesek B, Staskova Z, Lukas J, Rejthar A, Kovarik J, Midgley CA, Gannon JV, Lane DP: Aberrant expression of the p53 oncoprotein is a common feature of a wide spectrum of human malignancies. *Oncogene* 6: 1699–1703, 1991
26. Barisoni L, Kriz W, Mundel P, D'Agati V: The dysregulated podocyte phenotype: A novel concept in the pathogenesis of collapsing idiopathic focal segmental glomerulosclerosis and HIV-associated nephropathy. *J Am Soc Nephrol* 10: 51–61, 1999
27. Key G, Becker MH, Baron B, Duchrow M, Schluter C, Flad HD, Gerdes J: New Ki-67-equivalent murine monoclonal antibodies (MIB 1–3) generated against bacterially expressed parts of the Ki-67 cDNA containing three 62 base pair repetitive elements encoding for the Ki-67 epitope. *Lab Invest* 68: 629–636, 1993
28. Shankland SJ, Eitner F, Hudkins KL, Goodpaster T, D'Agati V, Alpers CE: Differential expression of cyclin-dependent kinase inhibitors in human glomerular disease: Role in podocyte proliferation and maturation. *Kidney Int* 58: 674–683, 2000
29. Wagrowska-Danilewicz M, Danilewicz M: A study of apoptosis in human glomerulonephritis as determined by in situ non-radioactive labelling of DNA strand breaks. *Acta Histochem* 99: 257–266, 1997
30. Kreidberg JA, Sariola H, Loring JM, Maeda M, Pelletier J, Housman D, Jaenisch R: WT-1 is required for early kidney development. *Cell* 74: 679–691, 1993
31. Mitra D, Jaffe EA, Weksler B, Hajjar KA, Soderland C, Laurence J: Thrombotic thrombocytopenic purpura and sporadic hemolytic-uremic syndrome plasmas induce apoptosis in restricted lineages of human microvascular endothelial cells. *Blood* 89: 1224–1234, 1997
32. Dang CT, Magid MS, Weksler B, Chadburn A, Laurence J: Enhanced endothelial cell apoptosis in splenic tissues of patients with thrombotic thrombocytopenic purpura. *Blood* 93: 1264–1270, 1999
33. Wyllie AH: Cell death: A new classification separating apoptosis from necrosis. In: *Cell Death in Biology and Pathology*, edited by Bowen ID, Lockshin RA, London, Chapman and Hall, 1981, pp 9–34
34. Buja LM, Eigenbrodt ML, Eigenbrodt EH: Apoptosis and necrosis. Basic types and mechanisms of cell death. *Arch Pathol Lab Med* 117: 1208–1214, 1993

35. Saraste A, Pulkki K: Morphologic and biochemical hallmarks of apoptosis. *Cardiovasc Res* 45: 528–537, 2000
36. Svendsen E, Jorgensen L: Focal “spontaneous” alterations and loss of endothelial cells in rabbit aorta. *Acta Pathol Microbiol Scand [A]* 86: 1–13, 1978
37. Feldman JD, Mardiney MR, Unanue ER, Cutting H: The vascular pathology of thrombotic thrombocytopenic purpura. An immunohistochemical and ultrastructural study. *Lab Invest* 15: 927–946, 1966
38. Kwaan HC: Clinicopathologic features of thrombotic thrombocytopenic purpura. *Semin Hematol* 24: 71–81, 1987
39. May P, May E: Twenty years of p53 research: Structural and functional aspects of the p53 protein. *Oncogene* 18: 7621–7636, 1999